JAAS

Accepted Manuscript

Accumulation and transformation of nanomaterials in ecological model organisms investigated by synchrotron radiation techniques

Yunyun Li [a,b], Yu-Feng Li[*, a], Jiating Zhao [a], Yuxi Gao [a], Chunying Chen [c]

[a] CAS Key Laboratory for Biomedical Effects of Nanomaterials and Nanosafety, Institute of High Energy Physics, Chinese Academy of Sciences, Beijing 100049, China

[b] University of Chinese Academy of Sciences, Beijing 100049, China

[c] CAS Key Laboratory for Biomedical Effects of Nanomaterials and Nanosafety, National Center for Nanoscience and Technology, Beijing 100190, China

*Corresponding auhtor: Email: liyf@ihep.ac.cn, Tel: +86-10-88233908, Fax: +86-10-88235294

TOC entry

Application of SR techniques to study the accumulation and transformation of engineered nanomaterials in different model organisms of the terrestrial, aquatic and atmospheric system.

Abstract

Engineered nanomaterials are promising in many aspects; however, information on the potential risks of the engineered nanomaterials to the ecological system is still limited. With wide frequency range and high brilliance, SR light sources are tunable, highly polarized, and pulsed. This made SR techniques achieve much improved signal to noise ratio, better spatial and temporal resolution and much reduced acquisition times than those using the conventional light sources. In this review, the application of SR techniques to study the accumulation and transformation of engineered nanomaterials was summarized using different model organisms in ecosystem including the terrestrial, aquatic and atmospheric system.

Introduction

Engineered nanomaterials, in the range of 1 to 100 nm, are promising in many aspects including drug delivery, environmental protection and consumer products etc.[1-3] Nanomaterials can be produced by naturally occurring processes including fire, volcanic activity, and erosion etc., However, the current magnitude of production of engineered nanomaterials warrant caution.[1, 4] In recent years, concerns about the possible adverse effects of engineered nanomaterials were raised and a new research field as nanotoxicology was formed. [2, 5-11] Engineered nanoparticles may enter the human body either directly in the manufacturing processes, use, and disposal of nano-products, or indirectly, by bio-magnification and enrichment via food chains following intentional releases such as soil and water remediation efforts.[12-18]

Besides, manufactured nanoparticles can also enter the environment unintentionally through domestic wastewater, atmospheric emissions, and accidental release during manufacture/transport.[19] Information on the potential risks of the engineered nanomaterials to the ecological system and whether nanomaterials will accumulate through the food chain and end up in higher-level organisms is still limited.[20] Ecological model organisms are extensively used to understand particular biological effects, with the expectation that discoveries made in organism models will provide insight into the workings of the ecological system.[21] Monitoring of the accumulation and transformation of nanomaterials in model organisms is essential to evaluate their effects to ecological systems.

Dedicated tools are necessary to investigate the accumulation and transformation of engineered nanomaterials in ecological model organisms. Several approaches can monitor the accumulation of nanomaterials: inductively coupled plasma optical emission spectroscopy (ICP-OES), inductively coupled plasma mass spectroscopy (ICP-MS), isotopic tracing (IT), neutron activation analysis (NAA), single-photon emission computed tomography (SPECT), positron emission tomography (PET), and magnetic resonance imaging (MRI).[11, 22] In general, ICP-MS, ICP-OES, IT and NAA require sacrificing the model organisms to get quantitative information for the nanomaterials. Although SPECT, PET, CT, and MRI can show the whole body distribution of nanoparticles directly, their quantification capability is limited.[11]

Synchrotron radiation (SR) facilities can produce tunable, highly polarized, wide frequency range (from infrared up to the highest-energy X-rays), pulsed (pulse durations at or below one nanosecond) and high brilliance light source (many orders of magnitude more than conventional X-ray tube sources). SR techniques are based on the detection of the absorption, the scattering or the secondary particles emissions excited by SR light source.[23] Among them, X-ray absorption fine Structure (XAFS) and soft/hard X-ray microscopy (scanning transmission X-ray microscopy, STXM; transmission X-ray microscopy, TXM) etc are based on the absorption of SR light by the samples; X-ray diffraction (XRD), and small angle X-ray scattering (SAXS) etc. are based the scattering of SR light by the samples; X-ray photoelectron spectroscopy (XPS), and X-ray fluorescence spectrometry (XRF) etc are based on the monitoring of the emission of the secondary particles excited by the SR light.[24, 25] The techniques that apply SR light source can greatly improve the signal to noise ratio, spatial and temporal resolution and reduce acquisition times than those using the conventional light source (for example, from the X-ray tubes), which makes SR techniques an outstanding tool in many scientific fields.[23, 26-36]

In this review, the application of SR techniques to study the accumulation and transformation of engineered nanomaterials will be summarized using model organisms in ecosystem including the terrestrial, aquatic and atmospheric system.

Terrestrial system

Plants

Plants, especially crops are an important component in the terrestrial system and may serve as a potential pathway for nanomaterials transport and a route for bioaccumulation into the food chain.

Soybeans are major global commodity crop, which provide more edible oil and protein than any other food crop. However, it was reported that soybeans may be exposed to engineered nanomaterials through the application of biosolids from wastewater treatment plants.[37] López-Moreno et al [38] studied the transformation of two high-production metal oxide nanomaterials (nano-CeO_2 and nano-ZnO) in soybeans by XAFS. XAFS is a technique to determine the local geometric and/or electronic structure of matter. The samples can be in the gas-phase, solution, or solid.[39, 40]

The Ce L_{III} edge XAFS spectra (Fig. 1A) revealed that soybean roots took up and stored nano CeO_2. Ce had the same oxidation state (IV) inside roots as in the nano CeO_2. The XANES spectra (Fig. 1B) from roots treated with 4000 mg nano-ZnO L^{-1}

showed that within tissues Zn was in the oxidation state of Zn(II) but not present as nano ZnO. Zn was coordinated in the same manner as Zn nitrate or Zn acetate. Therefore, nano CeO_2 was not transformed in roots whereas nano ZnO was transformed after uptake by roots. Besides, nano CeO_2 could also be up taken and remained as nano CeO_2 in the other plants, like alfalfa, corn, cucumber and tomato.[41] A further study proved that the absorbed nano CeO_2 could bring genotoxicity and diminish the plant growth and yield in the soybean plants. The nitrogen fixation process was found to be shut down at high nano CeO_2 concentration.[42] These findings forewarn the agriculturally associated human and environment risks from these used engineered nanomaterials.

Titanium dioxide nanoparticles (nano TiO_2) are another high-production nanomaterials, which are up to 2 million tons per year worldwide. Larue et al [43] examined the nano TiO_2 uptake and impact in wheat and rapeseed plantlets. In hydroponic conditions, wheat and rapeseed plantlets were exposed to 14 nm or 25 nm anatase nano TiO_2, either through root or leaf exposure. Synchrotron radiation-based micro X-ray fluorescence (μ-XRF) was used to evaluate Ti distribution in roots and leaves. XRF is the emission of characteristic "secondary" (or fluorescent) X-rays from a material that has been excited by X-rays.[32] Because each element produces X-rays at a unique set of energies, XRF allows non-destructive measurement of the elemental composition of materials.[31] μ-XRF installed at the most advanced third-generation synchrotron radiation sources could offer an excitation spot size of less than 0.15×0.15 μm^2, and detection limits range from 5×10^{-20} to 3.9×10^{-19} mol/μm^2, which corresponds to a few thousand atoms within an irradiated spot. [29, 44]

It was found that nano TiO_2 could be taken up and accumulated in these plantlets during both root and leaf exposure and that Ti content is higher in rapeseed than in wheat. It was found that nano TiO_2 exposure induced increased root elongation but did not affect germination, evapotranspiration, or plant biomass, suggesting that although nano-TiO_2 could be accumulated in plant but may only moderately impact the plant development.

Synchrotron-based soft X-ray microscopes or scanning transmission X-ray microscopes (STXM) can study the distribution of certain chemical elements at high spatial resolution.[45] One also has access to spectroscopic signals that reflect the chemical bonding state of major low Z constituents, without the disordered inelastic scattering background that is present in electron energy loss spectroscopy. It is thus possible to image whole, hydrated cells up to several micrometers in thickness with nanometer-scale resolution.[46] As the result of the development of a new nanofabrication process for Fresnel zone plate lenses, resolution has been improved to 10 nm or better.[46-49] The combined application of STXM coupled with XAFS can analyze thin samples *in situ* with a spatial resolution of better than 30 nm, with no need for prior chemical extraction or staining. This combination has been used to map the distribution and biotransformation of La_2O_3 nanoparticles (NPs) in cucumber (*Cucumis sativus*).[50] La_2O_3 NPs were found transformed to needle-like $LaPO_4$ nanoclusters in the intercellular regions of the cucumber roots. The dissolution of NPs at the root surface induced by the organic acids extruded from root cells was thought to play an important role in the phytotoxicity of La_2O_3 NPs.

Caenorhabditis elegans

Caenorhabditis elegans (*C. elegans*) is a free-living, transparent nematode (roundworm), about 1 mm in length, which lives in temperate soil environments. It is a famous model organism for the investigation of biological processes including genomics, cell biology, metabolism, aging, and toxicology, because of its well established biology, short generation time, large brood size, and readily available life traits.[51]

μ-XRF (with a spot size of 3×5 μm^2) was used to investigate the bioaccumulation of engineered copper nanoparticles (Cu NPs) in *C. elegans* [52]. It was found that exposure to Cu NPs can result in an obvious elevation of Cu and K levels and a change of bio-distribution of Cu in nematodes. Accumulation of Cu occurs in the head and at a location 1/3 of the way up the body from the tail compared to the unexposed control. In contrast, when the worm was exposed to Cu^{2+}, a higher amount of Cu was detected in other portions of its body, especially in its excretory cells and intestine. The nondestructive and multi-elemental μ-XRF provides an important tool for mapping the elemental distribution in the whole body of a single tiny nematode at low levels. However, μ-XRF cannot tell us whether the absorbed nano Cu had been metabolized or not in *C. elegans*.

The combination of μ-XRF and microbeam X-ray absorbance fine structure (μ-XAFS) can simultaneously provide information about the subcellular distribution and chemical species of metals of interest. Qu et al. investigated the uptake and biotransformation of quantum dots (QDs) by ingestion in the natural feeding environment and the subsequent fate and behavior of QDs in *C. elegans*. [53] Fig. 2 shows the combined application of different techniques, where μ-XRF was used to provide precise information with subcellular spatial resolution, high sensitivity, and simultaneous distributions of various elements, while the μ-XAFS technique was used for the analysis of the physicochemical changes of chemical species *in vivo*. Besides, laser scanning confocal microscopy was used to confirm the whole-body distribution of QDs. It was found that QDs taken up by ingestion can accumulate in the alimentary system and enter into adjacent intestinal cells after a short time exposure of 12 h. QDs separate from *E. coli* after ingestion, and their metabolic pathway is different from *E. coli* or other ingested materials. More importantly, collapse of the QDs core/shell structure and release of toxic cadmium elements was observed by comparing the optical fluorescence image with the μ-XRF mapping, and selenium oxidation during digestion was observed for the first time by the *in situ* μ-XAFS spectra derived from different points in the digestive tract. Furthermore, QDs were transferred from the alimentary system to the reproductive system and produced cumulative toxicity after long-term exposure. Similarly, the study on the effect of silver nanoparticles on *C. elegans* using μ-XAFS also found toxicity that was ascribed to the dissolved silver ions.[54]

Earthworms

Earthworms are ideal organism for use in soil toxicity, which are common in a wide range of soils that may represent 60–80% of the total soil biomass. Earthworms are classified into three main ecophysiological categories: (1) leaf litter- or compost-dwelling worms (called Epigeic) e.g. *Eisenia fetida* (*E. fetida*); (2) topsoil- or subsoil-dwelling worms that feed (on soil), burrow and cast within soil, creating horizontal burrows in upper 10–30 cm of soil (called Endogeics); and (3) worms that construct permanent deep vertical burrows which they use to visit the surface to obtain plant material for food, such as leaves (called Anecic), e.g. *Lumbricus terrestris* (*L. terrestris*).[55]

The acute toxicity of nano TiO_2 and ZnO to *E. fetida* in artificial soil systems was studied after a 7-day exposure at different concentrations.[56] It was found that both Ti and Zn levels increased along with increasing dose of nano TiO_2 and ZnO. The levels of Ti and Zn were about 8 and 12 times that in the control when the dose reached 5 g kg^{-1} soil. This study demonstrates that both TiO_2 and ZnO NPs exert harmful effects on *E. fetida* when their levels are higher than 1.0 g kg^{-1} in soil, and that the toxicity of ZnO NPs was higher than TiO_2.

To test the propensity of accumulation of TiO_2 nanocomposite (nano TiO_2), the earthworm *L. terrestris* was exposed to the nano TiO_2 for 7 days in water or 2–8 weeks in soil with the nanocomposite mixed either into food or soil at concentrations ranging from 0 to 100 mg kg^{-1}.[57] Apoptosis was then measured by immunohistochemistry and Ti distribution by μ-XRF. No mortality was found in *L. terrestris*, but μ-XRF showed an enhanced apoptotic frequency which was higher in the cuticule, intestinal epithelium and chloragogenous tissue than in the longitudinal and circular musculature. TiO_2 nanoparticles did not seem to cross the intestinal epithelium/chloragogenous matrix barrier to enter the coelomic liquid, or the cuticule barrier to reach the muscular layers. No bioaccumulation of TiO_2 nanocomposites was observed.

The accumulation and transformation of gold nanoparticles (Au NPs) to *E. fetida* in artificial soil has been studied by a combination of μ-XRF and μ-XAFS (Fig. 3).[58] It was found that the uptake of Au NPs and $HAuCl_4$ was clearly related to exposure concentration and was far greater for $HAuCl_4$ than for Au NPs. Au was distributed throughout the earthworm cross section. The regions with the greatest intensity tended to be within the gut. The μ-XAFS demonstrated the presence of Au metal in the earthworm tissues since the spectra for hotspots identified in the earthworm tissue were virtually identical to the spectra for Au metal. Therefore, Au could be taken up intact and remained so once internalized. Transmission electron microscopy analysis of the Au NP-exposed worms further proved the electron-dense areas in the gut epithelia matching the size of the respective NPs used, present either as single particles or as groups of two to seven particles within the cytoplasm. The results suggest that nanoparticles present in soil from activities such as biosolids application have the potential to enter terrestrial food webs.

Aquatic systems

The potential toxicity of nanoparticles to aquatic organisms is of interest given that increased commercialization will inevitably lead to inadvertent exposures to aquatic systems. Aquatic systems can be further divided into freshwater and saltwater. Several model organisms including *Daphnia magna*, *Danio rerio*, *Oryzias latipes*, *Oryzias melastigma* and *Corophium volutator* have been used, among which *Daphnia magna*, *Danio rerio*, and *Oryzias latipes* are freshwater models while *Oryzias melastigma* and *Corophium volutator* are saltwater models.

Daphnia magna

As a freshwater crustacean, *Daphnia magna* (*D. magna*) is widely used as a laboratory animal for testing toxicity due to its small size, relatively short life span, ease of culture and early maturation. [59] They are a vital connection in the food chain; between the algae that they consume and the ecologically and economically important fish that consume them, it is imperative to understand the toxic response of *D. magna* to nanoparticles. Therefore, *D. magna* is used by various organizations, including the OECD and US EPA as a bioindicator.[60]

To assess the potential impact that nanoparticles may have upon release into aquatic environments. Lovern et al. [59] prepared titanium dioxide (TiO_2) and fullerene (C_{60}) nanoparticles by filtration in tetrahydrofuran or by sonication. *D. magna* were exposed to the four solutions using US EPA 48-h acute toxicity tests. Transmission-electron microscopy was used to record the images of the particle solutions, and the median lethal concentration, lowest-observable-effect concentration, and no-observable-effect concentration were determined. Exposure to filtered C_{60} and filtered TiO_2 caused an increase in mortality with an increase in concentration, whereas fullerenes show higher levels of toxicity at lower concentrations. Furthermore, nano-TiO_2 at μg/L levels can cause significant acute phototoxicity to *D. magna* under natural solar radiation, which has considerable environmental implications.[61]

Applications for silver nanomaterials in consumer products are rapidly expanding, creating an urgent need for toxicological examination of the exposure potential and ecological effects of silver nanoparticles (Ag NPs). Poynton et al. examined the toxicogenomic responses of nanotoxicity in *D. magna* exposed to $AgNO_3$ and Ag NPs and found that the Ag NPs disrupted their distinct expression profile and major biological processes, including protein metabolism and signal transduction. [62]

Cadmium selenide quantum dots (QDs) capped with zinc sulfide have been used in the semiconductor industry and in cellular imaging. Their small size (<10 nm) suggests that they may be readily assimilated by exposed organisms. Jackson et al. [63] exposed *D. magna* to both red and green QDs and used μ-XRF to study the distribution of Zn and Se in the organism (Fig. 4). The QDs appeared to be confined to the gut, and there was no evidence of further assimilation into the organism. Zinc and Se fluorescence signals were highly correlated, suggesting that the QDs had not dissolved to any extent. There was no apparent difference between red and green QDs; i.e., there was no effect of QD size. 3D tomography confirmed that the QDs were exclusively in the gut area of the organism. It is possible that the QDs aggregated and were therefore too large to cross the gut wall.

Atmospheric systems

There is ample and consistent evidence for adverse health effects associated with increased concentrations of ambient fine and ultrafine aerosol particles (nanoparticles).

[64, 65] The study on the inhalation toxicity of nanoparticles arose from a study on airborne ultrafine particles. [66] Diesel engine exhaust is especially rich in nanoparticles that can penetrate deep into the lungs and have a large surface to volume ratio on which to carry toxic chemicals into the body. In addition, the engineered nano-CeO_2 has also been used as a fuel additive to improve the burning efficiency of fuels, thus reducing fuel consumption, greenhouse gases and particle numbers in vehicle exhaust. [67]

While the use of CeO_2 contributes to a reduction in particulate matter, it is necessary to demonstrate that it does not alter the intrinsic toxicity of particles or co-pollutants that are emitted in the exhaust and can enter atmospheric systems. [68] Atherosclerosis-prone apolipoprotein E knockout (ApoE−/−) mice were exposed by inhalation to diluted exhaust from an engine using diesel fuel containing cerium oxide nanoparticles (CeO_2 NPs), and no clear signs were found of altered hematological or pathological changes. However, levels of proinflammatory cytokines were modulated in a brain region and the liver following exposure to exhaust containing cerium oxide nanoparticles. [69] Investigation of the tissue distribution of CeO_2 NPs after inhalation exposure in rats found that approximately 10% of the inhaled dose was measured in lung tissue after a single exposure. [70] After a single 6-h exposure, a CeO_2 NP sample was also distributed to tissues other than the lung, such as the liver, kidney, and spleen and brain, testis, and epididymis. Repeated exposure to CeO_2 NPs resulted in a significant accumulation of the particles in the (extra)pulmonary tissues. After exposure to TiO_2 NPs, morphological changes, translocation within the lung, and deposition in alveolar macrophages and, to a lesser extent, in type-I pneumocytes was observed in rats. [71]

Besides, it was found that the user of cosmetics would be exposed to nanomaterials predominantly through nanoparticle-containing agglomerates larger than the 1–100 nm aerosol fraction. [72]

Drosophila melanogaster (*D. melanogaster*), known generally as the common fruit fly or vinegar fly, is widely used for biological research in studies of genetics, physiology, microbial pathogenesis and life history evolution. It is typically used because it is an animal species that is easy to care for, breeds quickly, and lays many eggs. [73] The distribution of CdSe@ZnS quantum dots（QDs）in adult *D. melanogaster* were characterized by μ-XRF (Fig. 5). [74] From Fig. 5, it can be seen that Cd, Se and Zn were concentrated in the intestinal and reproductive system, indicating that QDs could accumulate in the intestinal and reproductive system. Fluorescence signals were observed in the testis of stage-1 larva by the LSCM technique. The results indicate that the QDs could potentially impact placenta translocation and the reproductive system.

For the purpose of toxicity testing in *Drosophila melanogaster* (*D. melanogaster*), a simple and cost-effective nebulizer-based method was developed to deliver nanoparticles to the respiratory system. [75] Red fluorescent CdSe/ZnS nanoparticles were successfully delivered to the fly respiratory system and visualized by fluorescence microscopy. Citrate-capped gold nanoparticles (Au NPs) were also found to have a significant in vivo toxicity, eliciting clear adverse effects in *D. melanogaster*: a strong reduction of their life span and fertility, the presence of DNA fragmentation, and a significant over-expression of stress proteins. [76]

Conclusions and future perspectives

With wide frequency range and high brilliance, SR light sources are tunable, highly polarized, and pulsed. This made SR techniques achieve much improved signal to noise ratio, better spatial and temporal resolution and much reduced acquisition times than those using the conventional light source (for example, the X-ray tubes). Synchrotron radiation based XRF, especially the μ-XRF has a spatial resolution at micro-, or even nanometer level, which makes the direct observance of nanoparticles in the tissues like soybean roots and even the whole body tiny model organism like *C. elegans* possible. Besides, XRF is a nearly nondestructive technique, which brings less damage to the samples that other techniques like laser ablation inductive coupled plasma mass spectrometry (LA-ICP-MS) and particle-induced X-ray Emission (PIXE). XAFS is usually performed at SR facility, which requires less pretreatment to monitor the transformation of nanomaterials in the model organisms. The combination of XRF and XAS provides not only the biodistribution but also the transformation of nanomaterials in the model organisms, which is essential to understand the ecological effects of nanomaterials. Table 1 summarizes the SR techniques that were used in the study of the accumulation and transformation of nanomaterials in different ecological model organisms. Other SR techniques like XRD with a micro-size beam could detect the nanomaterials *in situ* while time-resolved measurements are also possible using SR beams, which can be applied to monitor the real time transformation of nanomaterials.[77-79]

Although SR techniques can play important roles in characterization of the ecological effects of nanomaterials, including the accumulation and transformation of nanomaterials in model organisms, the number of works applying SR techniques in ecotoxicology of nanomaterials is still relative small. For example, to the best of our knowledge, none work has been carried out on the accumulation and transformation of engineered nanomaterials in aquatic model organisms like zebra fish and medaka fish and other atmospheric model organisms using SR techniques. This may be ascribed to the limited access to SR facilities by nanotoxicologists.

Acknowledgement

This work was financially supported by National Natural Science Foundation of China (11205168, 11375213, and 11475196). Y-F Li gratefully acknowledges the support of K. C. Wong Education Foundation, Hong Kong and the Youth Innovation Promotion Association, Chinese Academy of Sciences (2011017). C Chen acknowledges the National Science Fund for Distinguished Young Scholars (11425520). Beam time allocation and staff support at BSRF, Beijing, China; SSRF, Shanghai, China and PF, KEK, Japan are highly appreciated.

References

1. Y. Zhao and H. Nalwa, *Nanotoxicology: Interactions of Nanomaterials with Biological Systems*, American Scientific Publishers. 2007.
2. Y. Zhao, G. Xing and Z. Chai, *Nat. Nanotechnol.*, 2008, **3**, 191-192.
3. P. Liu, W. Qi, Y. Du, Z. Li, J. Wang, J. Bi and W. Wu, *Sci. China Chem.*, 2014, **57**, 1483-1490.
4. J. Deng, D. Yu and C. Gao, *Sci. China Chem.*, 2013, **56**, 1533-1541.
5. V. L. Colvin, *Nat. Biotechnol.*, 2003, **21**, 1166-1170.
6. A. Nel, T. Xia, L. Madler and N. Li, *Science*, 2006, **311**, 622-627. DOI: 10.1126/science.1114397.
7. Y. Zhu and W. Li, *Sci. China Chem.*, 2008, **51**, 1021-1029. DOI: 10.1007/s11426-008-0120-6.

8. A. D. Maynard, R. J. Aitken, T. Butz, V. Colvin, K. Donaldson, G. Oberdorster, M. A. Philbert, J. Ryan, A. Seaton, V. Stone, S. S. Tinkle, L. Tran, N. J. Walker and D. B. Warheit, *Nature*, 2006, **444**, 267-269.

9. R. F. Service, *Science*, 2003, **300**, 243. DOI: 10.1126/science.300.5617.243a.

10. Y.-F. Li, J. Zhao, Y. Qu, Y. Gao, Z. Guo, Z. Liu, Y. Zhao and C. Chen, *Nanomedicine*, 2015, **11**, 1531-1549. DOI: 10.1016/j.nano.2015.04.008.

11. C. Chen, Y.-F. Li, Y. Qu, Z. Chai and Y. Zhao, *Chem. Soc. Rev.*, 2013, **42**, 8266-8303.

12. H. Wang, J. Wang, X. Deng, H. Sun, Z. Shi, Z. Gu, Y. Liu and Y. Zhao, *J. Nanosci. Nanotechnol.*, 2004, **4**, 1019-1024.

13. H. Meng, Z. Chen, G. M. Xing, H. Yuan, C. Y. Chen, F. Zhao, C. C. Zhang and Y. L. Zhao, *Toxicol. Lett.*, 2007, **175**, 102-110. DOI: 10.1016/j.toxlet.2007.09.015.

14. B. Wang, W. Feng, M. Wang, J. Shi, F. Zhang, H. Ouyang, Y. Zhao, Z. Chai, Y. Huang, Y. Xie, H. Wang and J. Wang, *Biol. Trace Elem. Res.*, 2007, **118**, 233-243.

15. J. Wang, C. Chen, H. Yu, J. Sun, B. Li, Y.-F. Li, Y. Gao, W. He, Y. Huang, Z. Chai, Y. Zhao, X. Deng and H. Sun, *J. Radioanal. Nucl. Chem.*, 2007, **272**, 527-531.

16. F. Lao, L. Chen, W. Li, C. Ge, Y. Qu, Q. Sun, Y. Zhao, D. Han and C. Chen, *ACS Nano*, 2009, **3**, 3358-3368. DOI: 10.1021/nn900912n.

17. H. Meng, G. Xing, B. Sun, F. Zhao, H. Lei, W. Li, Y. Song, Z. Chen, H. Yuan, X. Wang, J. Long, C. Chen, X. Liang, N. Zhang, Z. Chai and Y. Zhao, *ACS Nano*, 2010, **4**, 2773-2783. DOI: 10.1021/nn100448z.

18. W. Song, D. Shao, S. Lu and X. Wang, *Sci. China Chem.* , 2014, **57**, 1291-1299.

19. W.-x. Zhang and D. W. Elliott, *Remed. J.*, 2006, **16**, 7-21. DOI: 10.1002/rem.20078.

20. V. J. Pansare, S. Hejazi, W. J. Faenza and R. K. Prud'homme, *Chem. Mater.*, 2012, **24**, 812-827. DOI: 10.1021/cm2028367.

21. S. Fields and M. Johnston, *Science*, 2005, **307**, 1885-1886. DOI: 10.1126/science.1108872.

22. C. Chen, Z. Chai and Y. Gao, *Nuclear Analytical Techniques for Metallomics and Metalloproteomics*, RSC Publishing, Cambridge. 2010.

23. L. Ma and F. Yang, *Introduction to the Applications of Synchrotron Radiation*, Fudan Universtiy Press, Shanghai. 2001.

24. Y.-F. Li, J. Zhao, Y. Li, X. Xu, L. Cui, B. Zhang, S. Shan, Y. Geng, J. Li, B. Li and Y. Gao, *Sci. China Chem.*, 2015, **45**, 597-613.

25. Z. Mai, *Synchrotron Radiation Light Source and its Applications*, Science Press, Beijing. 2013.

26. S. Nuzzo, M. H. Lafage-Proust, E. Martin-Badosa, G. Boivin, T. Thomas, C. Alexandre and F. Peyrin, *J. Bone Miner. Res.*, 2002, **17**, 1372-1382.

27. Y. Qin, C. Fan, Q. Huang and H. Chen, *Sci. China Chem.*, 2010, **20**, 22-30.

28. I. Snigireva and A. Snigirev, *J. Environ. Monitor.*, 2006, **8**, 33-42.

29. B. S. Twining, S. B. Baines, N. S. Fisher, J. Maser, S. Vogt, C. Jacobsen, A. Tovar-Sanchez and S. A. Sa udo-Wilhelmy, *Anal. Chem.*, 2003, **75**, 3806-3816.

30. P. Willmott, *An Introduction to Synchrotron Radiation: Techniques and Applications*, Wiley. 2011.

31. P. M. Bertsch and D. B. Hunter, *Chem. Rev.*, 2001, **101**, 1809-1842. DOI: 10.1021/cr990070s.

32. B. De Samber, G. Silversmit, R. Evens, K. De Schamphelaere, C. Janssen, B. Masschaele, L. Van Hoorebeke, L. Balcaen, F. Vanhaecke, G. Falkenberg and L. Vincze, *Anal. Bioanal. Chem.*, 2008, **390**, 267-271. DOI: 10.1007/s00216-007-1694-0.

33. Y.-F. Li, J. Zhao, Y. Li, H. Li, J. Zhang, B. Li, Y. Gao, C. Chen, M. Luo, R. Huang and J. Li, *Plant*

Soil, 2015, **391**, 195-205. DOI: 10.1007/s11104-015-2418-4.

34. J. Zhao, Y. Pu, Y. Gao, X. Peng, Y. Li, X. Xu, B. Li, N. Zhu, J. Dong, G. Wu and Y.-F. Li, *J. Anal. At. Spectrom.*, 2015, **30**, 1408-1413.

35. X. He, Y. Ma, M. Li, P. Zhang, Y. Li and Z. Zhang, *Small*, 2013, **9**, 1482-1491. DOI: 10.1002/smll.201201502.

36. Y. Zhu, X. Cai, J. Li, Z. Zhong, Q. Huang and C. Fan, *Nanomed. Nanotechnol. Biol. Med.*, 2014, **10**, 515-524. DOI: http://dx.doi.org/10.1016/j.nano.2013.11.005.

37. V. C. Currie, J. S. Angle and R. L. Hill, *Agric. Ecosys. Environ.*, 2003, **97**, 345-351. DOI: http://dx.doi.org/10.1016/S0167-8809(03)00134-8.

38. M. L. López-Moreno, G. de la Rosa, J. Á. Hernández-Viezcas, H. Castillo-Michel, C. E. Botez, J. R. Peralta-Videa and J. L. Gardea-Torresdey, *Environ. Sci. Technol.*, 2010, **44**, 7315-7320. DOI: 10.1021/es903891g.

39. R. Stumm von Bordwehr, *Ann. Phys. Fr.*, 1989, **14**, 377-465.

40. D. Koningsberger and R. Prins, *X-ray absorption: principles, applications, techniques of EXAFS, SEXAFS and XANES*, Wiley. 1987.

41. M. L. López-Moreno, G. de la Rosa , J. A. Hernández-Viezcas, J. R. Peralta-Videa and J. L. Gardea-Torresdey, *J. Agr. Food Chem.*, 2010, **58**, 3689-3693. DOI: 10.1021/jf904472e.

42. J. H. Priester, Y. Ge, R. E. Mielke, A. M. Horst, S. C. Moritz, K. Espinosa, J. Gelb, S. L. Walker, R. M. Nisbet, Y.-J. An, J. P. Schimel, R. G. Palmer, J. A. Hernandez-Viezcas, L. Zhao, J. L. Gardea-Torresdey and P. A. Holden, *Proc. Natl Acad. Sci. USA*, 2012, **109**, E2451–E2456. DOI: 10.1073/pnas.1205431109.

43. Larue C, Veronesi G, Flank AM, Surble S, Herlin-Boime N and C. M, *J. Toxicol. Environ. Health*, 2012, **75**, 722-734.

44. R. McRae, P. Bagchi, S. Sumalekshmy and C. Fahrni, *J. Am. Chem. Soc.*, 2009, **131**, 12497-12515.

45. J. Maser, A. Osanna, Y. Wang, C. Jacobsen, J. Kirz, S. Spector, B. Winn and D. Tennant, *J. Microsc.*, 2000, **197**, 68-79.

46. W. Chao, J. Kim, S. Rekawa, P. Fischer and E. H. Anderson, *Opt. Expr.*, 2009, **17**, 17669-17677.

47. G. McDermott, M. A. Le Gros and C. A. Larabell, in *Ann. Rev. Phys. Chem.*, ed. M. A. Johnson and T. J. Martinez. 2012, vol. 63, pp. 225-239.

48. M. Uchida, G. McDermott, M. Wetzler, M. A. Le Gros, M. Myllys, C. Knoechel, A. E. Barron and C. A. Larabell, *Proc. Natl Acad. Sci. USA*, 2009, **106**, 19375-19380. DOI: 10.1073/pnas.0906145106.

49. W. Chao, B. D. Harteneck, J. A. Liddle, E. H. Anderson and D. T. Attwood, *Nature*, 2005, **435**, 1210-1213.

50. Y. Ma, X. He, P. Zhang, Z. Zhang, Z. Guo, R. Tai, Z. Xu, L. Zhang, Y. Ding, Y. Zhao and Z. Chai, *Nanotoxicology*, 2011, **5**, 743-753. DOI: doi:10.3109/17435390.2010.545487.

51. C. A. Wolkow, K. D. Kimura, M.-S. Lee and G. Ruvkun, *Science*, 2000, **290**, 147-150. DOI: 10.1126/science.290.5489.147.

52. Y. Gao, N. Liu, C. Chen, Y. Luo, Y.-F. Li, Z. Zhang, Y. Zhao, Y. Zhao, A. Iida and Z. Chai, *J. Anal. At. Spectrom.*, 2008, **23**, 1121-1124.

53. Y. Qu, W. Li, Y. Zhou, X. Liu, L. Zhang, L. Wang, Y.-f. Li, A. Iida, Z. Tang, Y. Zhao, Z. Chai and C. Chen, *Nano Lett.*, 2011, **11**, 3174-3183. DOI: 10.1021/nl201391e.

54. X. Yang, A. P. Gondikas, S. M. Marinakos, M. Auffan, J. Liu, H. Hsu-Kim and J. N. Meyer, *Environ. Sci. Technol.*, 2011, **46**, 1119-1127. DOI: 10.1021/es202417t.

55. K. E. Lee, *Earthworms: Their Ecology and Relationships with Soils and Land Use*, Academic Press, Sydney. 1985.

56. C. Hu, M. Li, Y. Cui, D. Li, J. Chen and L. Yang, *Soil Biol. Biochem.*, 2010, **42**, 586-591.

57. E. Lapied, J. Y. Nahmani, E. Moudilou, P. Chaurand, J. Labille, J. Rose, J.-M. Exbrayat, D. H. Oughton and E. J. Joner, *Environ. Int.*, 2011, **37**, 1105-1110. DOI: http://dx.doi.org/10.1016/j.envint.2011.01.009.

58. J. M. Unrine, S. E. Hunyadi, O. V. Tsyusko, W. Rao, W. A. Shoults-Wilson and P. M. Bertsch, *Environ. Sci. Technol.*, 2010, **44**, 8308-8313. DOI: 10.1021/es101885w.

59. S. B. Lovern and R. Klaper, *Environ. Toxicol. Chem.*, 2006, **25**, 1132-1137. DOI: 10.1897/05-278R.1.

60. R. D. Combes, I. Gaunt and M. Balls, *Alternatives Lab. Animals*, 2004, **32**, 163-208.

61. H. Ma, A. Brennan and S. A. Diamond, *Environ. Toxicol. Chem.*, 2012, **31**, 1621-1629. DOI: 10.1002/etc.1858.

62. H. C. Poynton, J. M. Lazorchak, C. A. Impellitteri, B. J. Blalock, K. Rogers, H. J. Allen, A. Loguinov, J. L. Heckman and S. Govindasmawy, *Environ. Sci. Technol.*, 2012, **46**, 6288-6296. DOI: 10.1021/es3001618.

63. B. Jackson, H. Pace, A. Lanzirotti, R. Smith and J. Ranville, *Anal. Bioanal. Chem.*, 2009, **394**, 911-917. DOI: 10.1007/s00216-009-2768-y.

64. N. L. Mills, H. Törnqvist, M. C. Gonzalez, E. Vink, S. D. Robinson, S. Söderberg, N. A. Boon, K. Donaldson, T. Sandström, A. Blomberg and D. E. Newby, *N. Engl. J. Med.*, 2007, **357**, 1075-1082. DOI: doi:10.1056/NEJMoa066314.

65. C. A. Pope, *N. Engl. J. Med.*, 2004, **351**, 1132-1134. DOI: doi:10.1056/NEJMe048182.

66. G. Oberdorster, E. Oberdorster and J. Oberdorster, *Environ. Health Perspect.*, 2005, **113**, 823-839. DOI: 10.1289/ehp.7339.

67. B. Park, K. Donaldson, R. Duffin, L. Tran, F. Kelly, I. Mudway, J.-P. Morin, R. Guest, P. Jenkinson, Z. Samaras, M. Giannouli, H. Kouridis and P. Martin, *Inhal. Toxicol.*, 2008, **20**, 547-566. DOI: doi:10.1080/08958370801915309.

68. F. R. Cassee, E. C. van Balen, C. Singh, D. Green, H. Muijser, J. Weinstein and K. Dreher, *Critical Rev. Toxicol.*, 2011, **41**, 213-229. DOI: doi:10.3109/10408444.2010.529105.

69. F. R. Cassee, A. Campbell, A. J. F. Boere, S. G. McLean, R. Duffin, P. Krystek, I. Gosens and M. R. Miller, *Environ. Res.*, 2012, **115**, 1-10. DOI: http://dx.doi.org/10.1016/j.envres.2012.03.004.

70. L. Geraets, A. G. Oomen, J. D. Schroeter, V. A. Coleman and F. R. Cassee, *Toxicol. Sci.*, 2012, **127**, 463-473. DOI: 10.1093/toxsci/kfs113.

71. M. Eydner, D. Schaudien, O. Creutzenberg, H. Ernst, T. Hansen, W. Baumgärtner and S. Rittinghausen, *Inhal. Toxicol.*, 2012, **24**, 557-569. DOI: doi:10.3109/08958378.2012.697494.

72. Y. Nazarenko, H. Zhen, T. Han, P. J. Lioy and G. Mainelis, *Environ. Health Perspect.*, 2012, **120**, 885.

73. E. C. R. Reeve and I. Black, *Encyclopedia of Genetics*, Taylor & Francis Group. 2001.

74. H. Liu, B. Wang, Z. Wang, M. Li, Y. Kang, X. Bi, X. Yu and W. Feng, *Nucl. Tech.*, 2011, **34**, 415-418.

75. R. Posgai, M. Ahamed, S. M. Hussain, J. J. Rowe and M. G. Nielsen, *Sci. Total Environ.*, 2009, **408**, 439-443. DOI: http://dx.doi.org/10.1016/j.scitotenv.2009.10.008.

76. P. Pompa, G. Vecchio, A. Galeone, V. Brunetti, S. Sabella, G. Maiorano, A. Falqui, G. Bertoni and R. Cingolani, *Nano Res.*, 2011, **4**, 405-413. DOI: 10.1007/s12274-011-0095-z.

77. E. Lombi and J. Susini, *Plant Soil*, 2009, **320**, 1-35. DOI: 10.1007/s11104-008-9876-x.

78. X.-F. Shen, Y.-S. Ding, J. C. Hanson, M. Aindow and S. L. Suib, *J. Am. Chem. Soc.*, 2006, **128**, 4570-4571.

79. Q. Wu, L. D. L. Duchstein, G. L. Chiarello, J. M. Christensen, C. D. Damsgaard, C. F. Elkjær, J. B. Wagner, B. Temel, J.-D. Grunwaldt and A. D. Jensen, *ChemCatChem*, 2014, **6**, 301-310. DOI: 10.1002/cctc.201300628.

Figure captions

Fig.1 A）XANES L_{III}-edge spectra (5723 eV) of CeO_2 NPs, CeN_3O_9 model compounds, and spectra from soybean roots germinated in 4000 mg/L of CeO_2 NPs, B) XANES K-edge spectra (9659 eV) of ZnO NPs, Zn $(NO_3)_2$, and Zn $(O_2CCH_3)_2$ model compounds and spectra from soybean roots germinated in 4000 mg/L of ZnO NPs. (Reproduced with permission from ACS [38])

Fig. 2 *In situ* elemental analysis of metabolism of QDs in *C. elegans* by μ-XRF and μ-XAS. Optical fluorescence of QDs (QDs Fluor.) versus selenium μ-XRF map of an intact worm exposed to MEA-CdSe@ZnS for 24h. *In situ* Se K edge microbeam X-ray absorption fine structure (μ-XAFS) spectra of QDs within the digestive tract of *C. elegans* corresponded to points A, B, and C on XRF map. The beam size of μ-XRF map and μ-XAFS spectra was 5 × 5 μm^2. (Reproduced with permission from RSC [11]).

Fig. 3 A) μ-XAFS (fluorescence mode) of Au foil and $HAuCl_4$ standards compared to μ-XAFS from foci located within tissues of earthworms and samples of soil fortified with either $HAuCl_4$, 20nm Au nanoparticles or 55 nm Au nanoparticles. B) μ-XRF graphs showing the spatial localization of Au in cross sections of earthworms exposed to either $HAuCl_4$, 20 nm Au NPs or 55 nm Au nanoparticles. The graphs transect a 0.8 mm wide region from the body wall (bottom) to the gut (top). The region located at 0.8, 0.4 mm in the 20 nm micrograph contained high concentrations of Ti and was likely a soil particle. C) Regions of interest in the tissue cross sections represented in the scan are shown outlined in red in the light micrographs of the tissue sections. (Reproduced with permission from the ACS [58])

Fig. 4 Optical images (*left*) and corresponding Ca, Zn, Se elemental overlay by μ-XRF for 24-h QDs exposures. (Reproduced with permission from Springer [63])

Fig. 5 Distribution of Cd, Se and Zn by μ-XRF in the CdSe@ZnS QDs-exposed adult fruit flies. [74]

527 # Figures

528 Fig.1

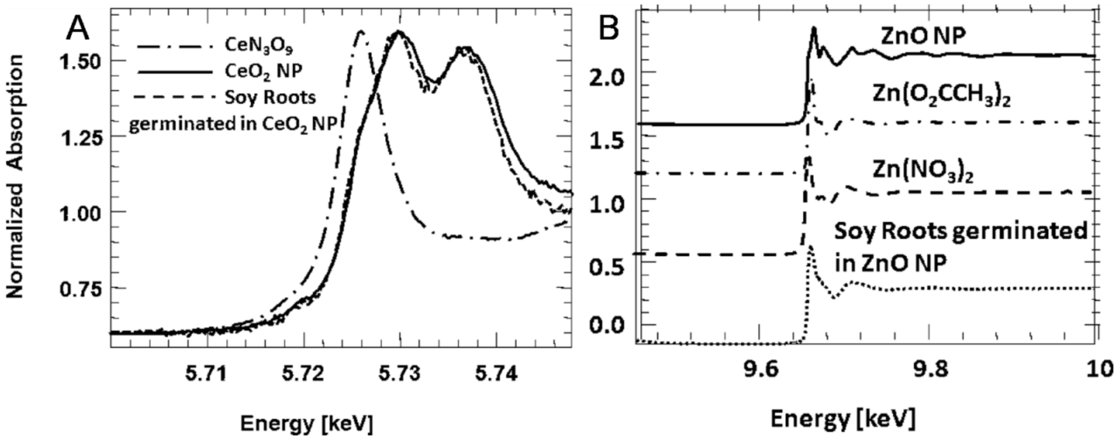

529

530

Fig. 2

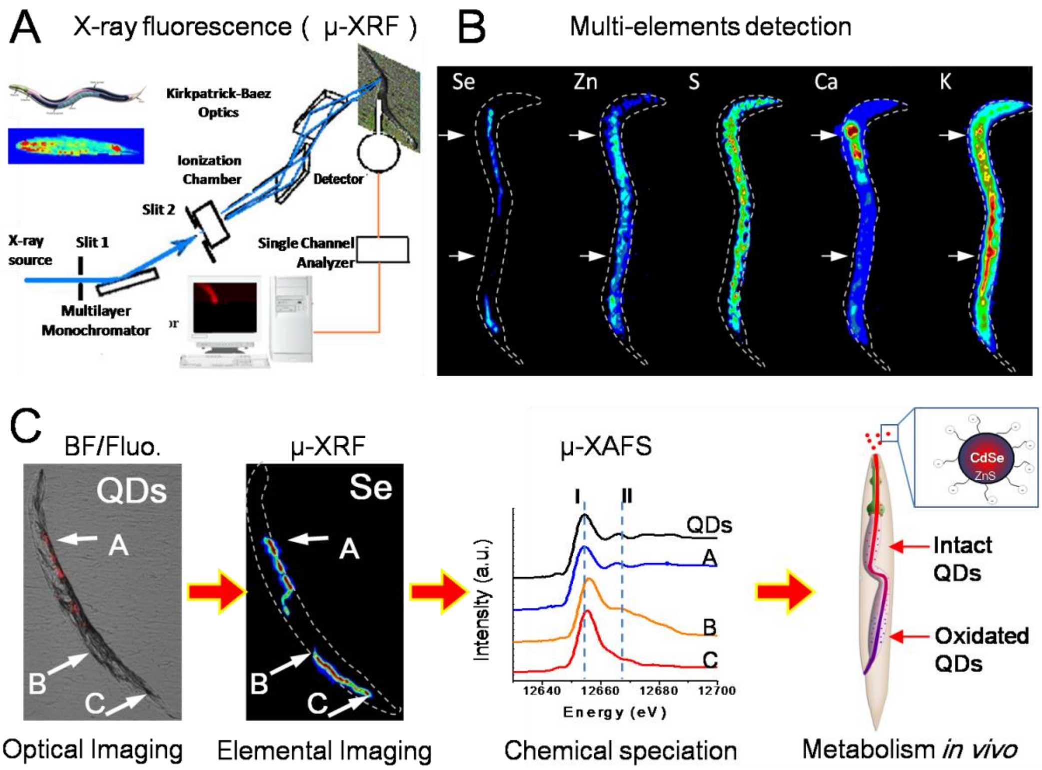
A X-ray fluorescence (μ-XRF)
Kirkpatrick-Baez Optics
Ionization Chamber
Detector
Slit 2
X-ray source
Slit 1
Single Channel Analyzer
Multilayer Monochromator
B Multi-elements detection
Se
Zn
S
Ca
K
C
BF/Fluo.
QDs
A
B
C
μ-XRF
Se
μ-XAFS
I
II
QDs
Intensity (a.u.)
12640
12660
12680
12700
Energy (eV)
CdSe
ZnS
Intact QDs
Oxidated QDs
Optical Imaging
Elemental Imaging
Chemical speciation
Metabolism *in vivo*

Fig. 3

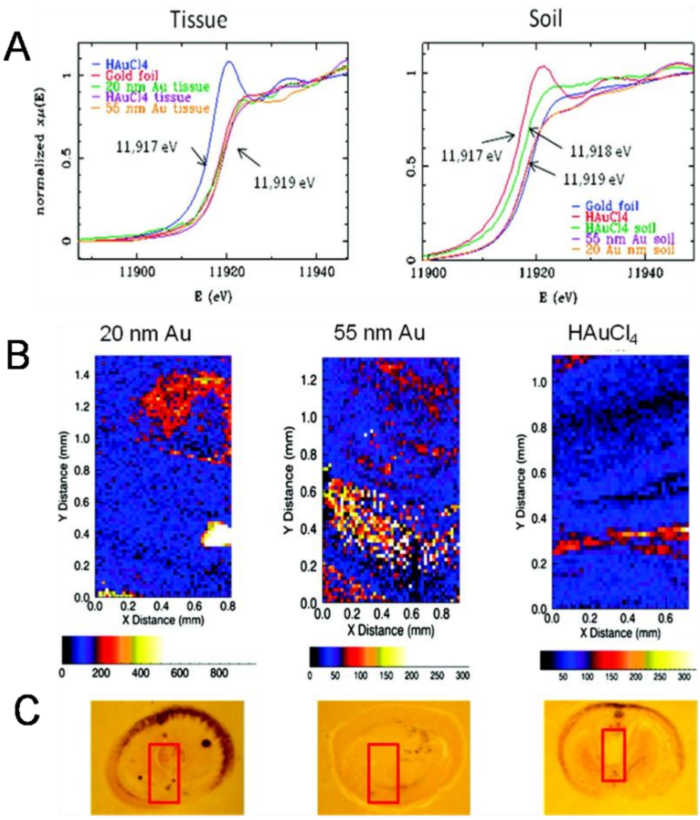
A
Tissue
Soil
normalized xμ(E)
HAuCl4
Gold foil
20 nm Au tissue
HAuCl4 tissue
55 nm Au tissue
11,917 eV
11,919 eV
11,918 eV
HAuCl4 soil
55 nm Au soil
20 Au nm soil
E (eV)
B
20 nm Au
55 nm Au
HAuCl4
Y Distance (mm)
X Distance (mm)
C

Fig. 4

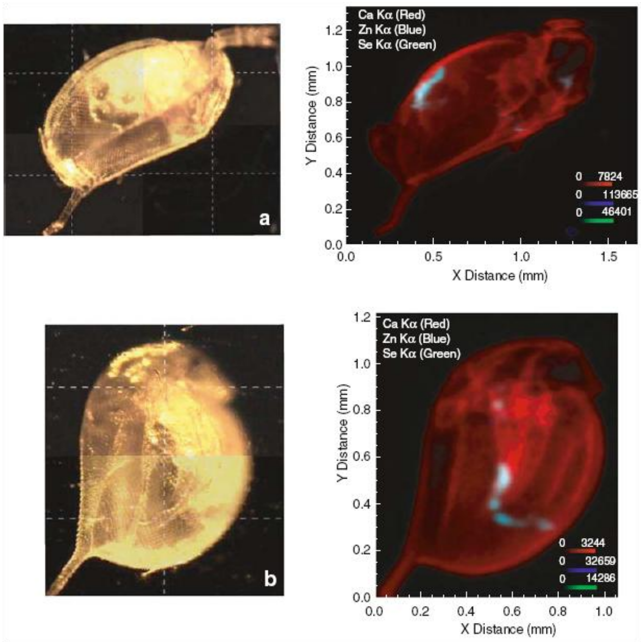
a
Ca Kα (Red)
Zn Kα (Blue)
Se Kα (Green)
Y Distance (mm)
X Distance (mm)
0 7824
0 113665
0 46401
b
Ca Kα (Red)
Zn Kα (Blue)
Se Kα (Green)
Y Distance (mm)
X Distance (mm)
0 3244
0 32659
0 14286

Fig. 5

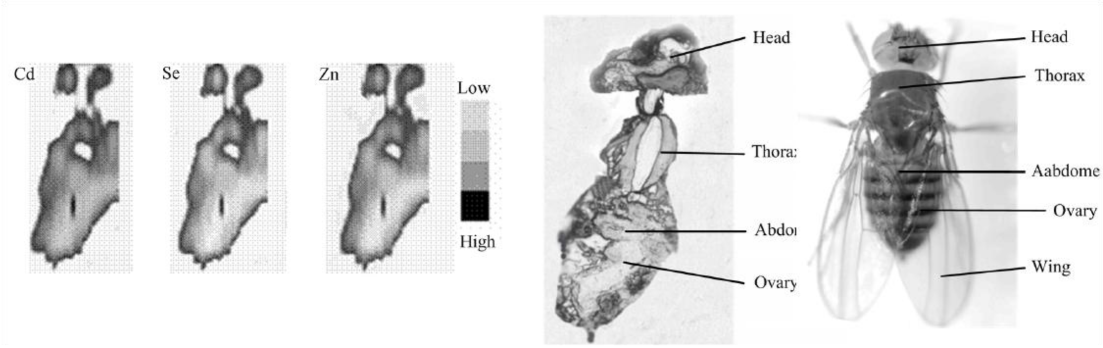

Tables

Table 1 Summary of SR techniques that were used in the study of the accumulation and transformation of nanomaterials in different ecological model organisms

Ecological systems	Model organisms		Nanomaterials	SR techniques	References
Terrestrial	Plants	Soybeans	CeO_2, ZnO	XAFS	36
		Rapeseed	TiO_2	μ-XRF	41
		Cucumber	La_2O_3	STXM, XAFS	48
	C. elegans		Cu	μ-XRF	50
			QDs	μ-XRF, μ-XAFS	51
	L. terrestris		TiO_2	μ-XRF	55
	E. fetida		Au	μ-XRF, μ-XAFS	56
Aquatic	*D. magna*		QDs	μ-XRF	61
Atmospheric	*D. melanogaster*		QDs	μ-XRF	72